forests

MDPI

Article

Changes in Soil Substrate and Microbial Properties Associated with Permafrost Thaw Reduce Nitrogen Mineralization

Xue Yang [1,2], Xiaoying Jin [1,2,*], Sizhong Yang [3], Huijun Jin [1,2,4,*], Hongwei Wang [1,4], Xiaoying Li [2,5,6], Ruixia He [6], Junfeng Wang [6], Zhizhong Sun [6,7] and Hanbo Yun [6,8,9]

1 School of Civil Engineering and Transportation, Permafrost Institute, China-Russia Joint Laboratory of Cold Regions Engineering and Environment, Northeast Forestry University, Harbin 150040, China; yangx014@nenu.edu.cn (X.Y.); wanghw@lzb.ac.cn (H.W.)
2 Scientific Observation and Research Station of Permafrost and Cold-Regions Environment in the Da Xing'anling Mountains, Northeast China, Natural Resources Institute of Heilongjiang Province, Harbin 150036, China; lixiaoying@nefu.edu.cn
3 Cryosphere Research Station on the Qinghai-Tibet Plateau, Northwest Institute of Eco-Environment and Resources, Chinese Academy of Sciences, Lanzhou 730000, China; yangsz@lzb.ac.cn
4 Key Laboratory of Remote Sensing of Gansu Province, Northwest Institute of Eco-Environment and Engineering, Chinese Academy of Sciences, Lanzhou 730000, China
5 Ministry of Education Key Laboratory of Sustainable Forest Ecosystem Management, School of Forestry, Northeast Forestry University, Harbin 150040, China
6 State Key Laboratory of Frozen Soil Engineering, Northwest Institute of Eco-Environment and Resources, Chinese Academy of Sciences, Lanzhou 730000, China; ruixiahe@lzb.ac.cn (R.H.); wangjf2008@lzb.ac.cn (J.W.); sun@lzb.ac.cn (Z.S.); hbyun@lzb.ac.cn (H.Y.)
7 Da Xing'anling Observation and Research Station of Frozen Ground Engineering and Environment, Northwest Institute of Eco-Environment and Resources, Chinese Academy of Sciences, Jiagedaqi 165000, China
8 Center for Permafrost (CENPERM), Department of Geosciences and Natural Resource Management, University of Copenhagen, DK1350 Copenhagen, Denmark
9 Department of Earth, Atmospheric, and Planetary Sciences, Purdue University, West Lafayette, IN 47906, USA
* Correspondence: xyj@nefu.edu.cn (X.J.); hjjin@nefu.edu.cn (H.J.)

Citation: Yang, X.; Jin, X.; Yang, S.; Jin, H.; Wang, H.; Li, X.; He, R.; Wang, J.; Sun, Z.; Yun, H. Changes in Soil Substrate and Microbial Properties Associated with Permafrost Thaw Reduce Nitrogen Mineralization. *Forests* **2023**, *14*, 2060. https://doi.org/10.3390/f14102060

Academic Editor: Heinz Rennenberg

Received: 29 August 2023
Revised: 5 October 2023
Accepted: 7 October 2023
Published: 16 October 2023

Abstract: Anticipated permafrost thaw in upcoming decades may exert significant impacts on forest soil nitrogen (N) dynamics. The rate of soil N mineralization (N_{min}) plays a crucial role in determining soil N availability. Nevertheless, our understanding remains limited regarding how biotic and abiotic factors influence the N_{min} of forest soil in response to permafrost thaw. In this study, we investigated the implications of permafrost thaw on N_{min} within a hemiboreal forest based on a field investigation along the degree of permafrost thaw, having monitored permafrost conditions for eight years. The results indicate that permafrost thaw markedly decreased N_{min} values. Furthermore, N_{min} demonstrated positive associations with soil substrates (namely, soil organic carbon and soil total nitrogen), microbial biomass carbon and nitrogen, and soil moisture content. The decline in N_{min} due to permafrost thaw was primarily attributed to the diminished quality and quantity of soil substrates rather than alterations in plant community composition. Collectively, our results underscore the pivotal role of soil substrate and microbial biomass in guiding forest soil N transformations in the face of climate-induced permafrost thaw.

Keywords: permafrost thaw; nitrogen mineralization; soil organic carbon and nitrogen; microbial biomass; forests

1. Introduction

Defined as ground that remains at temperatures of 0 °C or below for a minimum of two years, permafrost encompasses roughly 22% of the exposed land surface in the northern hemisphere [1]. Over the span from 2007 to 2016, a noticeable uptick in global permafrost temperatures occurred, registering an increase of approximately 0.29 ± 0.12 °C, attributed primarily to climatic warming trends [2]. This warming phenomenon has subsequently led to a notable degradation in and the warming of permafrost regions [3]. As permafrost undergoes thawing, the once entrapped soil organic matter (SOM) becomes vulnerable to microbial breakdown [4]. Consequently, the rates at which soil nitrogen is mineralized (N_{min}) are postulated to rise, furnishing an enhanced nitrogen replenishment to plant systems, which can potentially mitigate plant nutrient deficits [5]. Given that heightened nitrogen accessibility might bolster plant growth, thereby offsetting carbon losses due to SOM breakdown, grasping the nuances of N_{min} influence amidst permafrost thaw has become paramount for forecasting carbon trajectories in impacted locales.

Nitrogen (N) is vital for both plants and soil microbes. However, permafrost systems usually face nitrogen limitations [6]. Some research results indicate that permafrost thaw elevates N_{min}, releasing significant amounts of available N in the recent changing climate [7,8].Upon permafrost thaw, N_{min} can be modulated by soil physicochemical properties, microbial characteristics, and plant community composition. Specifically, thawing permafrost releases labile SOM from deeper sediments, favoring N_{min} [9]. Concentrations of soil organic carbon (SOC) and soil total nitrogen (TN) predominantly regulate gross ammonification and nitrification processes [10]. Changes in microbial communities within the expanding active layer, attributed to permafrost thaw, may influence N_{min} [11]. Permafrost-affected soils are rich in microbial communities involved in mineral nutrient cycling, evident in both the active layer [12,13] and the permafrost strata [14]. The active layer thickness (ALT) and nitrogen inputs collectively determine plant community compositions and traits [15,16], and these factors exhibit a correlation with N_{min} [17]. In warming environments, plant species with elongated roots demonstrate a competitive edge. Furthermore, plant composition and growth patterns exhibit a significant correlation with both permafrost thaw and alterations in nitrogen availability [18]. The interplay among soil substrate, microbiome, and plant community can further affect N_{min} in those regions of thawing permafrost. However, prior research primarily focused on these factors individually. A holistic comprehension of their relative significance and influences on N_{min} in permafrost domains remains absent. Moreover, the effects of these factors on N_{min} might be distinct along a permafrost thaw gradient, such as varying ALTs, due to differences in soil properties, SOMs, microbial biomass, and plant community compositions during permafrost degradation phases [19–21]. Yet, the distinct roles of these factors in areas with permafrost thaw remain ambiguous.

Positioned in Northeast China, the Da Xing'anling Mountains forms the southeastern boundary of the East Asian permafrost belt [22–24]. Over the course of recent years, both climatic shifts and human interventions have been catalysts for substantial permafrost degradation in this specific region [23,25]. Such degradation is evidenced by changes in ALT, shifts in soil properties, modifications in microbial dynamics, and transitions in plant community patterns [26–28]. To delve deeper into the intricacies of N_{min} fluctuations and their shaping factors, our team collected soil samples from stable, attached permafrost zones and from those showing signs of degradation. This collection followed an eight-year observation of permafrost thermal patterns in the northern sectors of the Da Xing'anling Mountains. Our investigation is poised to address two fundamental questions: (1) In what manner does permafrost thaw alter N_{min} dynamics? (2) Amid the transition from permafrost thaw to diverse ALTs, which elements emerge as primary controllers or influencers of N_{min}?

2. Materials and Methods

2.1. Study Area

Our research was conducted in the confines of the Nanwenghe National Wetlands Nature Reserve (N3WR), delineated by coordinates 125°07′55″–125°50′05″ E and 51°05′07″–51°39′24″ N, with elevations ranging from 500 to 800 m a. s. l. The N3WR lies cradled against the southern base of the Yile'huli Mountains, which is an eastern appendage of the Da Xing'anling Mountains in the northern Heilongjiang Province, Northeast China.

Owing to its geospatial positioning at the southernmost tip of the Eastern Asia permafrost domain, this reserve is particularly susceptible to hastened deterioration of its intermittent, warmer permafrost patches. The N3WR is under the influence of a temperate continental monsoon climate, marked by summers that are short-lived and warm, in stark contrast to its prolonged, chilly winter seasons. Records indicate a shift in the decadal average of annual air temperatures, transitioning from −4.2 °C in the 1980s [29] to a milder −2.3 °C by the 2010s [30]. Parallelly, the region receives an average annual precipitation of around 500 mm. Notably, snowfall accounts for 30%–40% of this annual precipitation, while the rest is rainfall primarily concentrated in the growth season spanning June to August. The forested landscape of the study area is dominated by trees typically found in the hemiboreal zone, such as the Xingan larch (*Larix gmelinii*) and white birch (*Betula platyphylla*).

2.2. Soil Sampling and Plant Community Survey

For our research, we pinpointed four unique locations, denoted as sites 1 ($ALT_{0.6}$), 2 ($ALT_{0.8}$), 3 ($ALT_{2.0}$), and 4 ($ALT_{2.5}$), each representing different extents of permafrost thawing (details in Table A1). We have been consistently observing the thermal states of the permafrost across these sites since the beginning of 2010. At every specified location, we set aside five plots, each measuring 10 × 10 m, summing up to a collective 20 plots for the study. From each designated plot, soil cores covering a depth from the surface to 40 cm were meticulously gathered at intervals of 10 cm. This yielded a total of 80 individual soil samples. To ensure representative sampling, acknowledging slight spatial inconsistencies, cores derived from a single plot were integrated to form one composite sample. Upon extraction, samples were promptly cooled and transported for lab evaluation. Here, they were sifted using a 2.0 mm mesh and subsequently split. One portion was conserved at 4 °C awaiting its physicochemical examination, whereas the other was set aside at −20 °C for upcoming incubation processes. Using a C/N analyzer (produced by Elementar, Langenselbold, Germany), we determined SOC and TN concentrations. Soil pH was evaluated using a mixture of soil and distilled water at a volume ratio of 1:2.5. ALT, representing the distance from the surface of topmost layer of mineral soil down to the permafrost table, was derived from borehole measurements and corroborated with ground temperature records.

Regarding the assessment of plant communities, specific details were gathered. For trees, attributes such as the species, the diameter measured at breast height (often referred to as DBH, taken at a standard height of 1.3 m), and spatial positioning were recorded for trees with a DBH at more than 5 cm. For the understory comprising herbaceous plants, we meticulously noted both the species present and their relative abundances. For this, we used a consistent 1 × 1 m quadrant set at the corners of each individual plot. Within these designated areas, details, such as the specific identity of shrub species and smaller trees, coupled with their respective DBH (typically falling between 1.0 and 5.0 cm), were systematically documented.

2.3. Soil Incubation and Measurements

Net nitrogen mineralization (N_{min}), a prevalent metric for gauging the equilibrium between mineralization and immobilization, was evaluated by incubating moistened soil samples (1:1 soil-to-deionized water ratio) at 25 °C over a 14-day anaerobic span. To determine the N_{min} value, we assessed the change in concentrations of nitrate (NO_3^--N) and ammonium (NH_4^+-N) from the beginning to the conclusion of the incubation period. These specific concentrations were precisely measured with the aid of an Alliance flow analyzer, a product of Alliance Flow Analyser, Futura, based in Frépillon, France.

The quantification of microbial biomass carbon (MBC) and nitrogen (MBN) was conducted through the application of the chloroform fumigation–extraction method, as outlined in previous studies [31,32]. The obtained extracts underwent a filtration process utilizing a 0.45 μm syringe filter, supplied by Schleicher and Schuell, Dassel, Germany, and they were subsequently stored in a refrigerated environment pending for further analysis. Analytical procedures were employed to determine dissolved organic carbon (DOC) and TN levels, utilizing a TOC/TN analyzer (Multi N/C 3100, Analytik, Jena, Germany). Subsequent comparisons of DOC and TN between treated and non-treated extracts facilitated the application of distinct correction coefficients, set at 0.45 for MBC and 0.54 for MBN, to accurately ascertain the respective values of MBC and MBN [31,33].

2.4. Statistical Analyses

Before proceeding with the analysis, all collected data were subjected to an assessment of normality, utilizing R software, specifically version 4.1.2, as a tool for executing the evaluations [34]. Various variables, including N_{min}, soil water content (SWC), soil pH, SOC, TN, MBC, and MBN, were systematically analyzed using linear mixed-effects model analyses. In this context, ALT and soil depth were treated as fixed parameters, while elevation was considered a random factor. The analytical process made use of the "lme" function, found within the "nlme" package [35]. Furthermore, to comprehend the intricate interrelationships among variables, such as N_{min}, SWC, soil pH, soil substrate parameters, and microbial biomass, a correlation matrix was thoughtfully constructed. This matrix analysis was implemented utilizing the "rcorr" function, part of the "Hmisc" package [36]. In order to elucidate shifts in the plant species community composition, permutational analyses of variance (PERMANOVA, utilizing 999 permutations) were conducted employing the "adonis" function, housed within the "vegan" package [37].

A comprehensive understanding of the potential influences, both direct and indirect, of parameters, including ALT, SWC, soil pH, soil substrates, microbial biomass, and plant community composition, on N_{min} was sought through the utilization of the Structural Equation Model (SEM). A conceptual framework, which aimed to delineate potential interconnections among these variables, was thoughtfully devised, drawing inspiration from the relevant literature (see Figure A1 for reference). Considering the complex correlations amongst these variables, a principal component analysis (PCA) was performed as an initial step, aiming to formulate a multivariate functional eigen vector for each category (refer to Table A2 for details). Subsequently, the main principal components (PC1), which encompassed between 55.66% and 91.64% of the original variable variations, were incorporated into the SEM [38,39]. The SEM model underwent incremental refinements by strategically excluding variables and covariances that were not deemed crucial, with the objective of achieving a representation that was both parsimonious and coherent, as assessed using the Akaike Information Criterion (AIC). The overall effectiveness of the SEM model was critically evaluated utilizing the χ^2 and Fisher's C tests. The SEM model was performed using linear mixed models ("lme" function of the nlme package 3.1.153), with soil depth and elevation as random factors (piecewiseSEM package 2.1.2) [40].

3. Results

3.1. Variations in N_{min}, Soil Physiochemical Properties, Microbial Biomass, and Vegetation

A coherent trend in soil N_{min} was evident across all four layers, manifesting an average decrement of 64% transitioning from sites $ALT_{0.6}$ to $ALT_{2.5}$. It is noteworthy that no discernible variations materialized across the quartet of sites with differing ALT levels within the 0–40 cm soil depth (refer to Table 1 and Figure 1a). In contrast, both SOC and TN contents unveiled clear variations layered-wise, observing the apex values at site $ALT_{0.6}$ and experiencing a subsequent decrease at the successive three ALT locales. SWC and pH exhibited pronounced fluctuations, introducing diverse trends across all strata. The average concentrations of SOC, TN, and SWC dwindled by 91%, 91%, and 72%, respectively, transitioning from site $ALT_{0.6}$ to $ALT_{2.5}$ (see Table 1 and Figure 1b,c). Soil pH predominantly lingered below 5, reaching a zenith at site $ALT_{2.5}$ and plummeting to a nadir at $ALT_{0.6}$ (refer to Table 1 and Figure 1e). Conversely, while MBC showcased minuscule variations among the disparate ALT levels within the permafrost area, a precipitous decline was observed concomitant with an increase in soil depth (see Table 1 and Figure 2a). Simultaneously, MBN exhibited a noticeable reduction alongside intensifying permafrost thaw, signaling a 24% decrease from $ALT_{0.6}$ to $ALT_{2.5}$ (consult Table 1 and Figure 2b). Plant community composition (NMDS1) evidenced variations across all four locales (refer to Table 1 and Figure A2).

Table 1. Results (F values) of LMM testing [a].

	N_{min}	SWC	pH	SOC	TN	MBC	MBN	NMDSplant
ALT	18.69 ***	65.49 ***	25.87 ***	214.74 ***	157.69 ***	0.76 ns	14.65 ***	15.54 ***
Soil depth	30.73 ***	3.16 *	1.08 ns	18.05 **	17.85 ***	4.94 *	9.74 ***	0 ns
ALT × soil depth	5.73 **	1.38 ns	2.19 ns	1.02 ns	3.6 ns	0.82 ns	4.08 **	0 ns

[a] Linear mixed-effects models (LMMs) tested the effects of active layer thickness (ALT), soil depth, and their interactions on N_{min}, soil water content (SWC), soil pH, soil organic carbon (SOC), total nitrogen (TN), microbial biomass carbon (MBC), microbial biomass nitrogen (MBN), and plant community composition (NMDSplant). * $p < 0.05$; ** $p < 0.01$; *** $p < 0.001$.

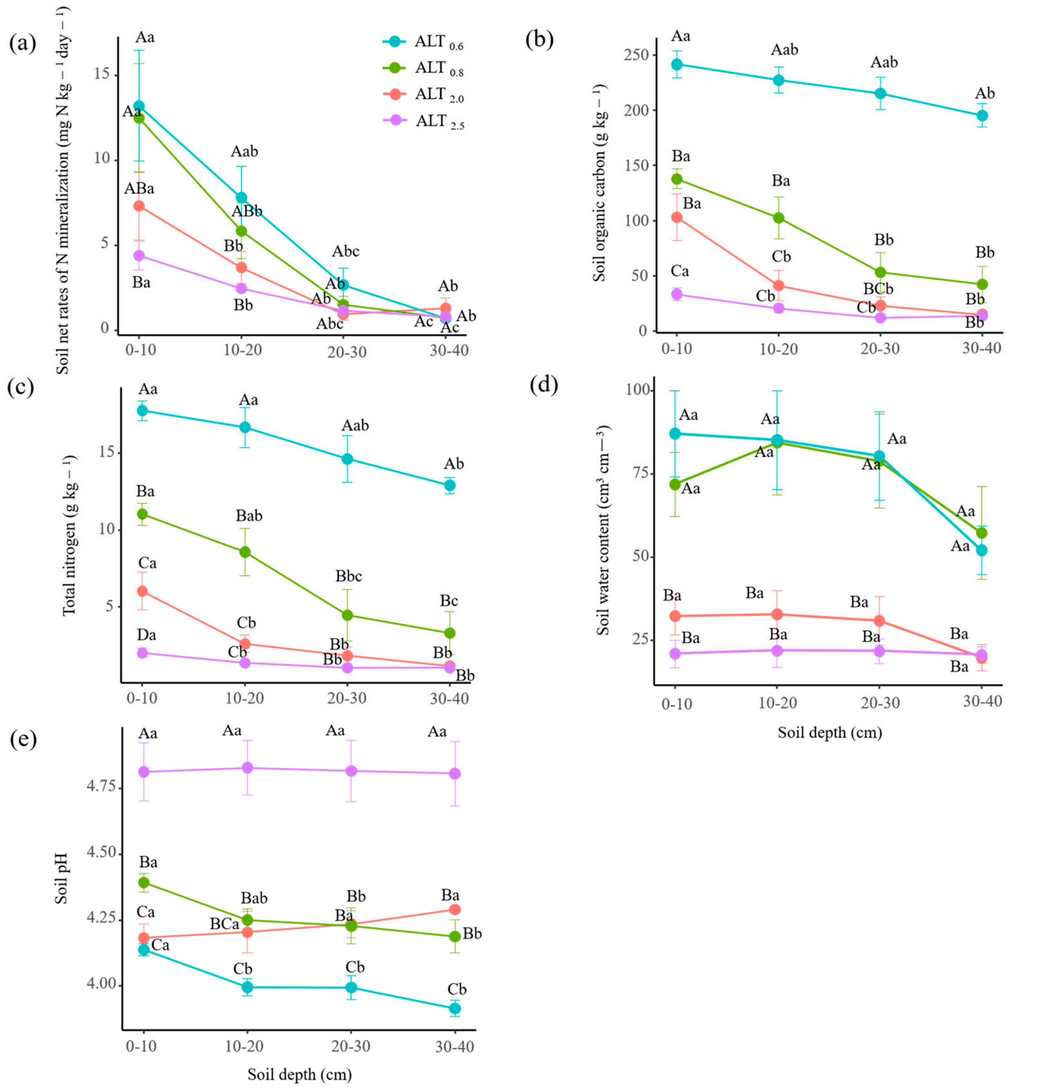

Figure 1. Depth gradients of soil net rates of N mineralization (N_{min}) (**a**), soil organic carbon (SOC) (**b**), total nitrogen (TN) (**c**), soil water content (SWC) (**d**), and soil pH (**e**) for the upper 40 cm soils among degree of permafrost thaw. Capital letters represent significant differences among the degree of permafrost thaw at the same soil depth. Lowercase letters represent significant differences among soil depth in the same degree of permafrost thaw.

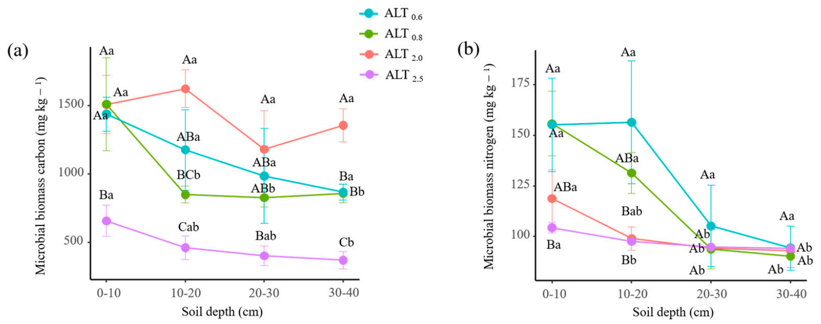

Figure 2. Depth gradients of microbial biomass carbon (MBC) (**a**) and microbial biomass nitrogen (MBN) (**b**) for the upper 40 cm soils among degree of permafrost thaw. Capital letters represent significant differences among the degree of permafrost thaw at the same soil depth. Lowercase letters represent significant differences among soil depth in the same degree of permafrost thaw.

3.2. Relationships among Vegetation, Soil Physicochemical Properties, Microbial Biomass, and N_{min}

Soil N_{min} forged a positive linkage with SWC and soil substrates, notably SOC and TN, along with microbial biomass indicators, such as MBC and MBN, a relationship clearly illustrated in Figure 3. Contrastingly, no perceptible correlation could be identified between N_{min} and other factors, which include pH, C/N, the ratio of MBC/MBN, and the composition of plant communities (NMDS1). SWC maintained a positive correlation with SOC, TN, and MBN, but it manifested a negative correlation when related to pH and the composition of plant communities (NMDS1). Simultaneously, pH was negatively associated with SOC, TN, MBC, and the MBC/MBN ratio, albeit displaying no noticeable correlation with the C/N ratio, MBN, or NMDS1. Moreover, both SOC and TN manifested positive associations with MBC and MBN while concurrently demonstrating a negative correlation with NMDS1.

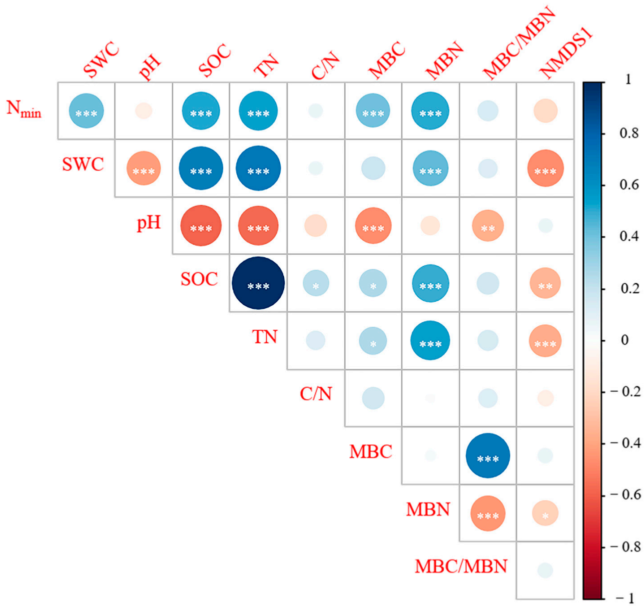

Figure 3. Correlations among N_{min}, soil water content (SWC), soil pH, soil substrate availability (SOC, TN, and C/N ratio), microbial biomass (MBC, MBN, and MBC/MBN ratio), and plant community composition (NMDS1) along permafrost thaw gradients. The orange boxes represent positive correlations, and blue boxes represent negative correlations. The sizes of colored circles indicate the strength of the correlation. * $p < 0.05$; ** $p < 0.01$; *** $p < 0.001$.

3.3. Direct and Indirect Effects of N_{min} Drivers

The utilization of Structural Equation Modeling (SEM) was undertaken to assess the direct and indirect implications of various explanatory variables on N_{min}, a relationship detailed graphically in Figure 4a. The models, meticulously constructed, elucidated 53% of the variability observed within the soil N_{min} (see Figure 4a for reference). The determining factors, such as SWC and pH, markedly molded the soil substrates and microbial biomass, which subsequently rose to prominence as pivotal determinants for N_{min}. When delving into the standardized total effects, as revealed via the SEM, it became evident that the primary forces for influencing N_{min} were notably the soil substrates. Subsequently, microbial biomass, SWC, pH, and ALT followed in significance, as delineated in Figure 4b.

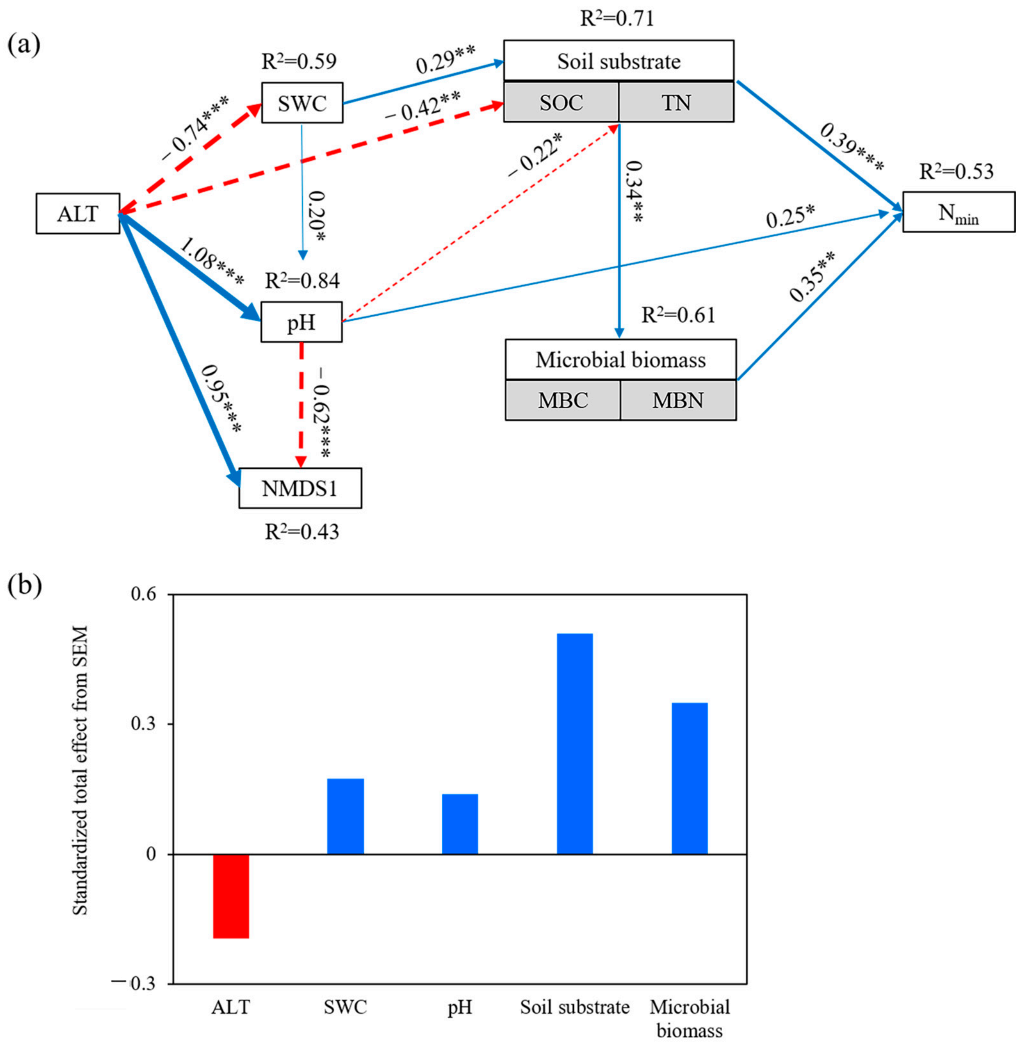

Figure 4. The Structural Equation Model (SEM), illustrating both direct and oblique consequences of several variables on N_{min}: ALT (indicative of permafrost thaw), soil water content (SWC), soil pH, availability of soil substrate (as informed by SOC and TN), microbial biomass (interpreted through MBC and MBN), and the composition of plant communities (NMDS1) (**a**), complemented by their standardized total impacts as extracted from the SEM (**b**). The delineation of relationships of significance is achieved through both unbroken (solid) and dashed lines. Pertinent goodness-of-fit statistics for the employed model include Fisher's = 13.099, $p = 0.786$, df = 18, with significance levels demarcated as * $p < 0.05$; ** $p < 0.01$; and *** $p < 0.001$. Directionality of influence between variables is represented through arrows, with accompanying numerical figures representing standardized path coefficients and arrow thickness illustrating the magnitude of said coefficients. Blue and red arrows represent positive and negative relationships, respectively.

In the depicted graphical model, associations of a positive nature are symbolized by arrows tinged in blue, while those of a negative character are highlighted using red arrows. Double-bordered rectangles are utilized to represent the first principal component (PC1), which was extracted from a meticulously conducted principal component analysis (PCA) focusing particularly on soil substrate availability and microbial biomass. Moreover, NMDS1 is representative of the initial component that was meticulously derived from the non-metric multidimensional scaling (NMDS), a process executed specifically for evaluating the composition of plant communities. Providing further clarity to the model, each response variable is accompanied by the coefficient of determination (R^2), which is purposefully integrated to articulate the fraction of the to-be-elucidated variance.

4. Discussion

This investigation provides a comprehensive examination into the determinants of N_{min} within regions impacted by permafrost, emphasizing on the nuanced interplay between both biotic and abiotic factors and delineating their respective impact pathways. The results elucidate a discernable decrease in N_{min} concurrent with the thawing of permafrost. Predominantly, soil substrate emerged as a critical factor, dictating the variability of N_{min} and sequentially influencing microbial communities within the soil. Furthermore, both SWC and soil pH, elements subject to fluctuation in tandem with alterations in e ALT, propagated their influences on N_{min} by modulating the soil substrate and microbial biomass. This inquiry illuminates the critical influence wielded by soil substrate and microbial entities in sculpting the nitrogen cycling within the soil and enhances our understanding of nitrogen cycling dynamics across regions impacted by permafrost. Through careful observation, it was indicated that changes in soil substrate and microbial biomass, instigated by the thawing of permafrost, may exert a considerable impact on ecosystem processes by modulating changes in N_{min}.

4.1. Changes in Soil Physiochemistry and Microbial Biomass with Permafrost Thaw

In stark contrast to the widely held notion asserting that the thawing of permafrost liberates additional SOC, TN, and dissolved inorganic nitrogen (DIN) into the active layer [8,41], the findings from our research instead propose that both SOC and TN contents experience a reduction concomitant with the amplification of permafrost thaw. It is noteworthy to mention that ALT within the Arctic permafrost region is substantially slimmer than its counterpart in the Da (Great) Xing'anling (Khinggan) Mountains in Northeast China [30,42,43]. Regions adjacent to the slimmer active layer, particularly in areas close to the permafrost table, witness a brisk release of SOC and TN into the surface soil, a phenomenon not observed in more remote areas. In these distant locales, swift releases into aquatic ecosystems through leaching or into the atmosphere via emissions transpire through processes, such as nitrification, denitrification (manifested as N_xO), and C mineralization (expressed as CH_4 and CO_2) [44,45], thereby diminishing SOC and TN in the active layer atop the thawing permafrost. Furthermore, a precipitous decline in SOC and TN contents is evident with increasing depth, potentially attributable to the enhanced input of leaf litter on surface soils, which fortifies SOM accumulation at relatively shallow depths in the active layer [46]. Additional contributing factors, such as the introduction of root litter, the secretion of root exudates, or an excess of N originating from the biological nitrogen fixation process, also perpetuate this observed trend [47].

A diminishing trend in MBC and MBN is discernible within our findings, particularly in the context of intensifying permafrost thaw. Despite existing research indicating that unstable permafrost constrains microbial biomass on the Qinghai–Tibet Plateau [48], contrasting observations were made in tundra where no notable variations in MBC or MBN were discerned amidst climate-triggered permafrost degradation [49]. The thawing process of permafrost enhances the availability of soil water, thereby influencing the diffusion rates of enzymes, degradation by-products, and substrates among microbes and their immediate micro-environment [50–53], which, in turn, instigates modifications within the soil microbial structure [54] and influences N availability. It is pivotal to highlight that a consistent microbial biomass implies that terrestrial ecosystems might not invariably demonstrate amplified sensitivity, especially in frigid regions [55,56]. Moreover, the declining trajectories of MBC and MBN with an increase in soil depth could potentially be correlated with the availability of oxygen and substrate in more profound soil strata, thus inhibiting the proliferation of aerobic microbial entities [57].

Regions characterized by resilient and stable permafrost exhibited a pronounced SWC in comparison to areas undergoing permafrost degradation. A correlation can be discerned wherein elevated SWC within zones of permafrost is associated with optimized vegetation development and an accumulation of SOM that surpasses that in talik areas, thereby impacting factors, such as soil water retention and heat conduction [58]. Upon the thawing of permafrost, the enhancement of soil drainage is affiliated with a reduction in SWC. Subsequent to this, distinct correlations are noted among SWC, SOC, and TN. Moreover, the induction of soil drainage, arid conditions, or drought through permafrost thaw is linked to an increase in soil pH. This relationship is substantiated by the observed inverse relationship between soil pH and SWC [59].

4.2. Drivers of Soil N Mineralization Rates (N_{min}) with Permafrost Thaw

A discernible decrease in N_{min} was documented at locations characterized by a comparatively thicker active layer, contrasting with those possessing a slimmer one. The rationale behind this observation can be fundamentally linked to the diminution in soil substrate, which transpires subsequent to thaw-induced soil drainage, a premise robustly substantiated by its emphatically positive correlation with N_{min}, as delineated in Figure 4. Key indicators instrumental in determining soil substrate, specifically SOC and TN, regulate N_{min} by exerting both direct and collateral impacts on microbial biomass, as visually represented in Figure 4. Previous investigative analyses established that the rates, at which processes, such as gross protein depolymerization, gross ammonification, and gross nitrification, occur, are intimately intertwined with SOC and TN concentrations, thereby affirming their pivotal role in orchestrating nitrogen turnover processes [10,60]. In a diverging observation, our data illustrated that the soil C/N ratio, which remained beneath the critical threshold of 20 [61], did not wield a significant influence over N_{min}. In a concordant vein, a meta-analysis has suggested that C:N stoichiometry does not invariably dictate N turnover across a spectrum of permafrost-impacted soils [10]. Moreover, SOM substantially influences the mobility of elemental complexes and governs bioavailability [62,63], wherein nutrient dissolution from complexes and bioavailable nutrient pools serve as pivotal factors for modulating soil microbial biomass and, concomitantly, their heterogeneous metabolic activities [64,65]. Microbial biomass stoichiometry and community composition exhibit variability in mediating soil nutrient mineralization [66,67]. In contrast with the gradual exposure of previously frozen organic matter through top-down permafrost thaw, abrupt permafrost thaw, for instance, via thermokarsting, unveils the entire soil column, not only influencing carbon and nitrogen stocks but also altering their chemical characteristics, thereby impacting mineralization rates [68]. Disturbed soils often exhibit heightened nitrogen mineralization, as undisturbed conditions preserve more SOM, with a significant portion of soil organic C and N sequestered within aggregates under natural field conditions [69]. The hierarchical structure of aggregates renders soil organic C and N less prone to soil microbial decomposition processes [70]. Consequently, permafrost thaw may engender conditions conducive to nitrification and denitrification, as observed on the Qinghai–Tibet Plateau [71].

The noted decrease in N_{min}, concurrent with ongoing permafrost thaw, might also find its explanation in the diminished microbial biomass. A considerable section of mineralizable nitrogen, which encompasses 55%–89% of its entirety, is theoretically derived from MBN [72], potentially providing a substantial substrate pivotal for N_{min}. The downward trajectory in microbial biomass potentially signals a dwindling presence of nitrogen-cycling microbial communities. Nevertheless, it is pivotal to acknowledge that a contraction in biomass does not invariably draw a parallel with a diminution in populations of specific functional groups. Permafrost degradation alters microbial diversity and community structure within the active layer, potentially by modifying microbial biomass and pH [73,74]. Moreover, the functional activities of microbes, predominantly the synthesis of soil extracellular enzymes, which play a pivotal role in the mineralization of large nitrogenous compounds, may witness a constraint subsequent to the thaw, attributed to the diminished microbial biomass [75,76]. An enhancement in microbial biomass could potentially act as a catalyst to invigorate microbial activity and proliferation, thereby fortifying N_{min} in the process.

Moreover, the observed decline of N_{min} as ALT increased could be potentially shaped by corresponding decreases in SWC. Fluctuations in SWC affect not only the soil substrate but also, by extension, the microbial biomass, thereby governing N_{min}. It is not uncommon for soils within the active layer in regions characterized by permafrost to remain saturated, or at least close to saturation, largely due to the restricting effect by permafrost exerted on the vertical migration of water [77]. Consequently, the precipitous loss of moisture through drainage during the thawing process, underlined by a notable 72% reduction in SWC identified in this study, has the capacity to exert detrimental effects on microbial communities, leading subsequently to the suppression of N_{min}.

Transformations in soil pH subsequent to thawing processes can also exert a diminishing effect on $N_{min.}$ The indirect modulation of N_{min} by soil pH occurs through its impact on the soil substrate and, subsequently, the microbial biomass, considering the crucial role that abundant SOM and TN play by providing vital nutrients conducive to microbial proliferation and metabolic activities [78]. In addition, the direct effect of soil pH on N_{min} may materialize through its regulation of microbial and enzymatic functions. To illustrate, certain enzymes, pivotal for optimal N_{min}, manifest their activity under conditions of acidity, and their functional activity may diminish when confronted with environments of elevated pH levels [79].

While plant communities hold the capacity to markedly influence N_{min} through the regulation of soil nutrient cycles, the findings from our research suggest that their role was not the predominant force following the thaw. These impacts may manifest indirectly and could be intermediated through alterations occurring in soil and microbial communities alike. A case in point is that lowland alder forests, when compared to lowland peatlands, demonstrated a notable enhancement in ammonification, a phenomenon potentially attributed to the additional substrate derived from alder detritus and the nitrogen introduced through the biological nitrogen fixation process [47]. Soil microbial communities, modulated by the quantity and quality of root exudates (e.g., the C/N ratio), can impact enzyme synthesis and soil N_{min} by facilitating the proliferation of fungal groups, given that slow-growing fungal groups possess the enzymatic capacity to decompose recalcitrant SOM and release labile N [80,81]. Moreover, deviations in the quantities and operational dynamics of soil microbes traversing vegetation gradients, exemplified by environments such as the Yellow River Delta [82], bear the potential to exert influence over N_{min}.

5. Conclusions

This research delved into the variances of N_{min} along a gradient of permafrost thaw within the boreal forests situated in Northeast China, placing a notable emphasis on soil substrate and microbial biomass as pivotal factors determining N_{min}. Contrarily, the composition of the plant community did not adequately illuminate the shifts in N_{min} observed across diverse ALT levels. In a broader context, the insights derived from our investigation suggest that permafrost thaw exerts a considerable impact on N_{min}, thereby potentially swaying the equilibrium of soil carbon and intricately weaving into the dynamic interactions between ecosystem nitrogen and carbon cycles amidst thawing occurrences.

Author Contributions: Conceptualization, X.Y., X.J. and H.J.; methodology, X.Y. and H.J.; software, X.Y. and R.H.; formal analysis, X.Y.; investigation, X.Y., X.J., X.L. and H.J.; writing—original draft preparation, X.Y., X.J., H.J., S.Y. and H.W.; writing—review and editing, X.Y., X.J., H.J., S.Y., H.W., X.L., R.H., J.W., Z.S. and H.Y. All authors have read and agreed to the published version of the manuscript.

Funding: This research was funded by the Natural Science Foundation of China (Grant Nos. 41771080, 42201139, and 42271155); Startup Funds of Northeast Forestry University for Chengdong Leadership (Grant No. LJ2020-01); Fundamental Research Fund for the Central Universities (Grant No. 2572021DT08); Heilongjiang Key Research and Development Program (Grant No. GZ20220103); China Postdoctoral Science Foundation (Grant No. 2022M710648); Heilongjiang Postdoctoral Foundation (Grant No. LBH-Z21088); the State Key Laboratory of Frozen Soils Engineering Open Fund (Grant No. SKLFSE202118); and the Danish National Research Foundation (Grant No. CENPERM DNRF 100).

Data Availability Statement: Data are available upon email request to the authors.

Acknowledgments: We would like to thank Gangyi Zhou, Fuqiang Che, Jipeng Wang, Lizhong Wang, Changlei Wei, Liming Liu, Huiren Li, Xikuan Zhao, Houkun Zhao, and Weidong Yu for their valuable help in field work.

Conflicts of Interest: The authors declare no conflict of interest.

Appendix A

Table A1. Sampling-point-related information.

Sample Sites	Coordinate	Elevation (m a.s.l.)	Plant	Active Layer Thickness (ALT) m
Site 1	125°08′10.000″ E 51°07′54.970″ N	445	*Carex tato* and shrubs	0.6
Site 2	125°08′09.911″ E 51°07′54.970″ N	445	*Carex tato*	0.8
Site 3	125°08′09.104″ E 51°07′44.776″ N	452	*Betula platyphylla* and *Larix gmelinii* (Rupr.) Kuzen	2.0
Site 4	125°08′16.943″ E 51°07′27.471″ N	474	*Larix gmelinii* (Rupr.) Kuzen	2.5

Table A2. Results of principle component analysis (PC1 and PC2) for soil substrate and microbial biomass.

Group	Variables	PC1 Score/%	PC2 Score/%
Soil substrate	SOC, TN	0.99	0.01
Microbial biomass	MBC, MBN	0.52	0.48

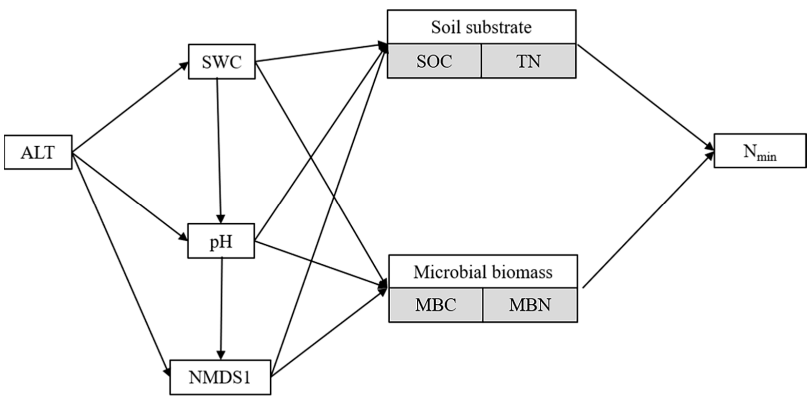

Figure A1. Hypothetical mechanisms of the individual paths in the Structural Equation Model. Arrows indicate the direction of the path.

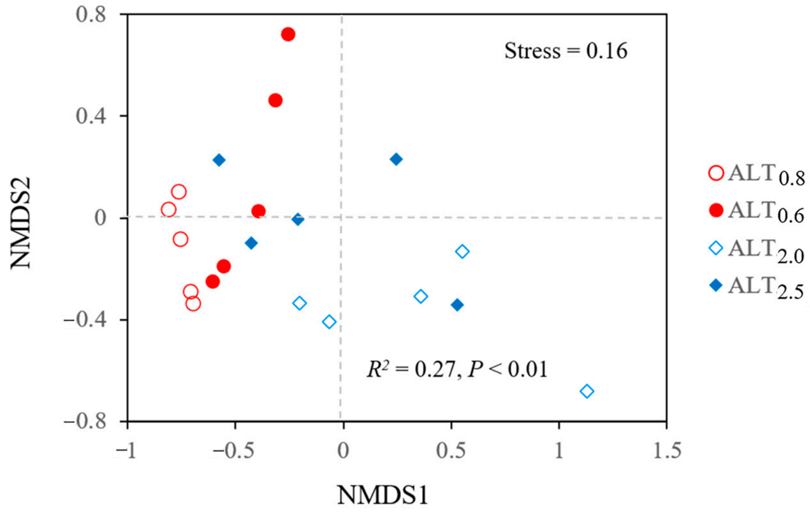

Figure A2. Non-metric multidimensional scaling (NMDS) of the plant community composition from $ALT_{0.6}$, $ALT_{0.8}$, $ALT_{2.0}$, and $ALT_{2.5}$. The ordination was performed with the Bray–Curtis dissimilarity matrix.

References

1. Obu, J.; Westermann, S.; Bartsch, A.; Berdnikov, N.; Christiansen, H.H.; Dashtseren, A.; Delaloye, R.; Elberling, B.; Etzelmüller, B.; Kholodov, A.; et al. Northern Hemisphere permafrost map based on TTOP modelling for 2000–2016 at 1 km^2 scale. *Earth-Sci. Rev.* **2019**, *193*, 299–316. [CrossRef]
2. Biskaborn, B.; Smith, S.; Noetzli, J.; Matthes, H.; Vieira, G.; Streletskiy, D.; Schoeneich, P.; Romanovsky, V.; Lewkowicz, A.; Abramov, A.; et al. Permafrost is warming at a global scale. *Nat. Commun.* **2019**, *10*, 264. [CrossRef]
3. Chadburn, S.E.; Burke, E.J.; Cox, P.M.; Friedlingstein, P.; Hugelius, G.; Westermann, S. An observation-based constraint on permafrost loss as a function of global warming. *Nat. Clim. Chang.* **2017**, *7*, 340–345. [CrossRef]
4. Schuur, E.A.; McGuire, A.D.; Schädel, C.; Grosse, G.; Harden, J.W.; Hayes, D.J.; Hugelius, G.; Koven, C.D.; Kuhry, P.; Lawrence, D.M.; et al. Climate change and the permafrost carbon feedback. *Nature* **2015**, *520*, 171–179. [CrossRef] [PubMed]
5. Kicklighter, D.W.; Melillo, J.M.; Monier, E.; Sokolov, A.P.; Zhuang, Q. Future nitrogen availability and its effect on carbon sequestration in Northern Eurasia. *Nat. Commun.* **2019**, *10*, 3024. [CrossRef] [PubMed]
6. Hobbie, S.E.; Nadelhoffer, K.J.; Högberg, P.A. Synthesis: The role of nutrients as constraints on carbon balances in boreal and arctic regions. *Plant Soil* **2002**, *242*, 163–170. [CrossRef]
7. Keuper, F.; van Bodegom, P.M.; Dorrepaal, E.; Weedon, J.T.; van Hal, J.; van Logtestijn, R.S.; Aerts, R. A frozen feast: Thawing permafrost increases plant-available nitrogen in subarctic peatlands. *Glob. Chang. Biol.* **2012**, *18*, 1998–2007. [CrossRef]
8. Salmon, V.G.; Soucy, P.; Mauritz, M.; Celis, G.; Natali, S.M.; Mack, M.C.; Schuur, E.A.G. Nitrogen availability increases in a tundra ecosystem during five years of experimental permafrost thaw. *Glob. Chang. Biol.* **2016**, *22*, 1927–1941. [CrossRef] [PubMed]
9. Rousk, K.; Michelsen, A.; Rousk, J. Microbial control of soil organic matter mineralization responses to labile carbon in subarctic climate change treatments. *Glob. Chang. Biol.* **2016**, *22*, 4150–4161. [CrossRef]
10. Ramm, E.; Liu, C.; Ambus, P.; Butterbach-Bahl, K.; Hu, B.; Martikainen, P.J.; Marushchak, M.E.; Mueller, C.W.; Rennenberg, H.; Schloter, M.; et al. A review of the importance of mineral nitrogen cycling in the plant-soil-microbe system of permafrost-affected soils-changing the paradigm. *Environ. Res. Lett.* **2022**, *17*, 013004. [CrossRef]
11. Mao, C.; Kou, D.; Chen, L.; Qin, S.; Zhang, D.; Peng, Y.; Yang, Y. Permafrost nitrogen status and its determinants on the Tibetan Plateau. *Glob. Chang. Biol.* **2020**, *26*, 5290–5302. [CrossRef] [PubMed]
12. Yergeau, E.; Hogues, H.; Whyte, L.G.; Greer, C.W. The functional potential of high Arctic permafrost revealed by metagenomic sequencing, qPCR and microarray analyses. *ISME J.* **2010**, *4*, 1206–1214. [CrossRef] [PubMed]
13. Alves, R.J.E.; Wanek, W.; Zappe, A.; Richter, A.; Svenning, M.M.; Schleper, C.; Urich, T. Nitrification rates in Arctic soils are associated with functionally distinct populations of ammonia-oxidizing archaea. *ISME J.* **2013**, *7*, 1620–1631. [CrossRef] [PubMed]
14. Hultman, J.; Waldrop, M.P.; Mackelprang, R.; David, M.M.; McFarland, J.; Blazewicz, S.J.; Harden, J.; Turetsky, M.R.; McGuire, A.D.; Shah, M.B.; et al. Multi-omics of permafrost, active layer and thermokarst bog soil microbiomes. *Nature* **2015**, *521*, 208–212. [CrossRef] [PubMed]
15. Keuper, F.; Dorrepaal, E.; van Bodegom, P.M.; van Logtestijn, R.; Venhuizen, G.; van Hal, J.; Aerts, R. Experimentally increased nutrient availability at the permafrost thaw front selectively enhances biomass production of deep-rooting subarctic peatland species. *Glob. Chang. Biol.* **2017**, *23*, 4257–4266. [CrossRef]
16. Standen, K.M.; Baltzer, J.L. Permafrost condition determines plant community composition and community-level foliar functional traits in a boreal peatland. *Ecol. Evol.* **2021**, *11*, 10133–10146. [CrossRef]

17. Fornara, D.A.; Tilman, D.; Hobbie, S.E. Linkages between plant functional composition, fine root processes and potential soil N mineralization rates. *J. Ecol.* **2009**, *97*, 48–56. [CrossRef]
18. Yun, H.; Zhu, Q.; Tang, J.; Zhang, W.; Chen, D.; Ciais, P.; Wu, Q.; Elberling, B. Warming, permafrost thawing and nitrogen availability are drivers of increasing plant growth and species richness on the Tibetan Plateau. *Soil Biol. Biochem.* **2023**, *182*, 109041. [CrossRef]
19. O'Donnell, J.A.; Jorgenson, M.T.; Harden, J.W.; McGuire, A.D.; Kanevskiy, M.Z.; Wickland, K.P. The effects of permafrost thaw on soil hydrologic, thermal, and carbon dynamics in an Alaskan peatland. *Ecosystems* **2012**, *15*, 213–229. [CrossRef]
20. Finger, R.A.; Turetsky, M.R.; Kielland, K.; Ruess, R.W.; Mack, M.C.; Euskirchen, E.S. Effects of permafrost thaw on nitrogen availability and plant-soil interactions in a boreal Alaskan lowland. *J. Ecol.* **2016**, *104*, 1542–1554. [CrossRef]
21. Che, L.; Cheng, M.; Xing, L.; Cui, Y.; Wan, L. Effects of permafrost degradation on soil organic matter turnover and plant growth. *Catena* **2022**, *208*, 105721. [CrossRef]
22. Jin, H.; Li, S.; Cheng, G.; Wang, S.; Li, X. Permafrost and climatic change in China. *Glob. Planet. Chang.* **2000**, *26*, 387–404. [CrossRef]
23. Jin, H.; Yu, Q.; Lu, L.; Guo, D.; He, R.; Yu, S.; Sun, G.; Li, Y. Degradation of permafrost in the Xing'anling Mountains, Northeastern China. *Permafr. Periglac. Process.* **2007**, *18*, 245–258. [CrossRef]
24. Jin, H.; Chang, X.; Luo, D.; He, R.; Lu, L.; Yang, S.; Guo, D.; Chen, X.; Harris, S.A. Evolution of permafrost in North east China since the late Pleistocene. *Sci. Cold Arid Reg.* **2016**, *84*, 269–296.
25. Zhang, Z.; Wu, Q.; Hou, M.; Tai, B.; An, Y. Permafrost change in Northeast China in the 1950s–2010s. *Adv. Clim. Chang. Res.* **2021**, *12*, 18–28. [CrossRef]
26. Jin, H.; Sun, G.; Yu, S.; Jin, R.; He, R. Symbiosis of marshes and permafrost in Da and Xiao Hinggan Mountains in North eastern China. *Chin. Geogr. Sci.* **2008**, *18*, 62–69. [CrossRef]
27. Chen, S.; Zang, S.; Sun, L. Characteristics of permafrost degradation in Northeast China and its ecological effects: A review. *Sci. Cold Arid. Reg.* **2020**, *12*, 1–11. [CrossRef]
28. Yang, L.; Zhang, Q.; Ma, Z.; Jin, H.; Chang, X.; Marchenko, S.S.; Spektor, V.V. Seasonal variations in temperature sensitivity of soil respiration in a larch forest in the Northern Daxing'an Mountains in Northeast China. *J. For. Res.* **2021**, *33*, 1061–1070. [CrossRef]
29. Zhou, Y.; Qiu, G.; Guo, D.; Cheng, G.; Li, S. *Geocryology in China*; Science Press: Beijing, China, 2000. (In Chinese) [CrossRef]
30. He, R.; Jin, H.; Luo, D.; Li, X.; Zhou, C.; Jia, N.; Jin, X.; Li, X.; Che, T.; Yang, X.; et al. Permafrost changes in the Nanwenghe Wetlands Reserve on the southern slope of the Da Xing'anling-Yile'huli mountains, Northeast China. *Adv. Clim. Chang. Res.* **2021**, *12*, 696–709. [CrossRef]
31. Brookes, P.C.; Landman, A.; Pruden, G.; Jenkinson, D.S. Chloroform fumigation and the release of soil nitrogen: A rapid direct extraction method to measure microbial biomass nitrogen in soil. *Soil Biol. Biochem.* **1985**, *17*, 837–842. [CrossRef]
32. Vance, E.D.; Brookes, P.C.; Jenkinson, D.S. An extraction method for measuring soil microbial biomass C. *Soil Biol. Biochem.* **1987**, *19*, 703–707. [CrossRef]
33. Joergensen, R.G.; Mueller, T. The fumigation-extraction method to estimate soil microbial biomass: Calibration of the kEN value. *Soil Biol. Biochem.* **1996**, *28*, 33–37. [CrossRef]
34. R Core Team. *R: A Language and Environment for Statistical Computing*; R Foundation for Statistical Computing: Vienna, Austria, 2021; Available online: https://www.R-project.org/ (accessed on 20 May 2022).
35. Pinheiro, J.; Bates, D.; DebRoy, S.; Sarkar, D. *nlme: Linear and Nonlinear Mixed Effects Models, R package version 3.1-153*; R Foundation for Statistical Computing: Vienna, Austria, 2021; Available online: https://CRAN.R-project.org/package=nlme\T1\textgreater{} (accessed on 21 January 2022).
36. Harrell, F.E., Jr. *Hmisc: Harrell Miscellaneous, R package version 4.6-0*; R Foundation for Statistical Computing: Vienna, Austria, 2021; Available online: https://CRAN.R-project.org/package=Hmisc (accessed on 22 February 2022).
37. Oksanen, J.; Blanchet, F.G.; Friendly, M.; Kindt, R.; Legendre, P.; McGlinn, D.; Minchin, P.R.; O'Hara, R.B.; Simpson, G.L.; Solymos, P.; et al. *vegan: Community Ecology Package, R package version 2.5-7*; R Foundation for Statistical Computing: Vienna, Austria, 2020; Available online: https://CRAN.R-project.org/package=vegan (accessed on 21 April 2021).
38. Liu, Y.; He, N.; Wen, X.; Xu, L.; Sun, X.; Yu, G.; Liang, L.; Schipper, L.A. The optimum temperature of soil microbial respiration: Patterns and controls. *Soil Biol. Biochem.* **2018**, *121*, 35–42. [CrossRef]
39. Wang, J.; Sun, J.; Yu, Z.; Li, Y.; Tian, D.; Wang, B.; Li, Z.; Niu, S. Vegetation type controls root turnover in global grasslands. *Glob. Ecol. Biogeogr.* **2019**, *28*, 442–455. [CrossRef]
40. Lefcheck, J.S. piecewiseSEM: Piecewise structural equation modeling in R for ecology, evolution, and systematics. *Methods Ecol. Evol.* **2016**, *7*, 573–579. [CrossRef]
41. Salmon, V.G.; Schädel, C.; Bracho, R.; Pegoraro, E.; Celis, G.; Mauritz, M.; Mack, M.C.; Schuur, E.A.G. Adding depth to our understanding of nitrogen dynamics in permafrost soils. *J. Geophys. Res-Biogeo.* **2018**, *123*, 2497–2512. [CrossRef]
42. Chang, X.; Jin, H.; Zhang, Y.; He, R.; Luo, D.; Wang, Y.; Lü, L.; Zhang, Q. Thermal impacts of boreal forest vegetation on active layer and permafrost soils in northern Da Xing'anling (Hinggan) Mountains, Northeast China. *Arct. Antarct. Alp. Res.* **2015**, *47*, 267–279. [CrossRef]
43. Aalto, J.; Karjalainen, O.; Hjort, J.; Luoto, M. Statistical forecasting of current and future circum-Arctic ground temperatures and active layer thickness. *Geophys. Res. Lett.* **2018**, *45*, 4889–4898. [CrossRef]

44. Voigt, C.; Marushchak, M.E.; Mastepanov, M.; Lamprecht, R.E.; Christensen, T.R.; Dorodnikov, M.; Jackowicz-Korczyński, M.; Lindgren, A.; Lohila, A.; Nykänen, H.; et al. Ecosystem carbon response of an Arctic peatland to simulated permafrost thaw. *Glob. Chang. Biol.* **2019**, *25*, 1746–1764. [CrossRef]
45. Voigt, C.; Marushchak, M.E.; Abbott, B.W.; Biasi, C.; Elberling, B.; Siciliano, S.D.; Sonnentag, O.; Stewart, K.J.; Yang, Y.; Martikainen, P.J. Nitrous oxide emissions from permafrost-affected soils. *Nat. Rev. Earth Env.* **2020**, *1*, 420–434. [CrossRef]
46. Jobbágy, E.G.; Jackson, R.B. The vertical distribution of soil organic carbon and its relation to climate and vegetation. *Ecol. Appl.* **2000**, *10*, 423–436. [CrossRef]
47. Ramm, E.; Liu, C.; Mueller, C.W.; Gschwendtner, S.; Yue, H.; Wang, X.; Bachmann, J.; Bohnhoff, J.A.; Ostler, J.; Schloter, J.; et al. Alder-induced stimulation of soil gross nitrogen turnover in a permafrost-affected peatland of Northeast China. *Soil Biol. Biochem.* **2022**, *172*, 108757. [CrossRef]
48. Wu, M.; Qu, D.; Li, T.; Liu, F.; Gao, Y.; Chen, S.; Chen, T. Effects of permafrost degradation on soil microbial biomass carbon and nitrogen in the Shule River headwaters, the Qilian Mountains. *Sci. Geogr. Sin.* **2021**, *41*, 177–186. (In Chinese) [CrossRef]
49. Xu, W.; Yuan, W. Responses of microbial biomass carbon and nitrogen to experimental warming: A meta-analysis. *Soil Biol. Biochem.* **2017**, *15*, 265–274. [CrossRef]
50. Davidson, E.A.; Samanta, S.; Caramori, S.S.; Savage, K. The Dual Arrhenius and Michaelis-M enten kinetics model for decomposition of soil organic matter at hourly to seasonal time scales. *Glob. Chang. Biol.* **2012**, *18*, 371–384. [CrossRef]
51. Manzoni, S.; Schimel, J.P.; Porporato, A. Responses of soil microbial communities to water stress: Results from a meta-analysis. *Ecology* **2012**, *93*, 930–938. [CrossRef]
52. Sistla, S.A.; Moore, J.C.; Simpson, R.T.; Gough, L.; Shaver, G.R.; Schimel, J.P. Long-term warming restructures Arctic tundra without changing net soil carbon storage. *Nature* **2013**, *497*, 615–618. [CrossRef] [PubMed]
53. Xu, W.; Yuan, W.; Dong, W.; Xia, J.; Liu, D.; Chen, Y. A meta-analysis of the response of soil moisture to experimental warming. *Environ. Res. Lett.* **2013**, *8*, 044027. [CrossRef]
54. Deslippe, J.R.; Hartmann, M.; Simard, S.W.; Mohn, W.W. Long-term warming alters the composition of Arctic soil microbial communities. *FEMS Microbiol. Ecol.* **2012**, *82*, 303–315. [CrossRef]
55. Lu, M.; Zhou, X.; Yang, Q.; Luo, Y.; Fang, C.; Chen, J.; Yang, X.; Li, B. Responses of ecosystem carbon cycle to experimental warming: A meta-analysis. *Ecology* **2013**, *94*, 726–738. [CrossRef]
56. Zhang, X.; Shen, Z.; Fu, G. A meta-analysis of the effects of experimental warming on soil carbon and nitrogen dynamics on the Tibetan Plateau. *Appl. Soil Ecol.* **2015**, *87*, 32–38. [CrossRef]
57. Xu, X.; Thornton, P.E.; Post, W.M. A global analysis of soil microbial biomass carbon, nitrogen and phosphorus in terrestrial ecosystems. *Glob. Ecol. Biogeogr.* **2013**, *22*, 737–749. [CrossRef]
58. Wu, X.; Fang, H.; Zhao, Y.; Smoak, J.M.; Li, W.; Shi, W.; Sheng, Y.; Zhao, L.; Ding, Y. A conceptual model of the controlling factors of soil organic carbon and nitrogen densities in a permafrost-affected region on the eastern Qinghai-Tibetan Plateau. *J. Geophys. Res.-Biogeo.* **2017**, *122*, 1705–1717. [CrossRef]
59. Xie, Y.; Zhang, J.; Meng, L.; Müller, C.; Cai, Z. Variations of soil N transformation and N2O emissions in tropical secondary forests along an aridity gradient. *J. Soil. Sediment.* **2015**, *15*, 1538–1548. [CrossRef]
60. Elrys, A.S.; Ali, A.; Zhang, H.; Cheng, Y.; Zhang, J.; Cai, Z.C.; Müller, C.; Chang, S.X. Patterns and drivers of global gross nitrogen mineralization in soils. *Glob. Chang. Biol.* **2021**, *27*, 5950–5962. [CrossRef] [PubMed]
61. Mooshammer, M.; Wanek, W.; Haemmerle, I.; Fuchslueger, L.; Hofhansl, F.; Knoltsch, A.; Schnecker, J.; Takriti, M.; Watzka, M.; Wild, B.; et al. Adjustment of microbial nitrogen use efficiency to carbon: Nitrogen imbalances regulates soil nitrogen cycling. *Nat. Commun.* **2014**, *5*, 3694. [CrossRef] [PubMed]
62. Fageria, N.K.; Baligar, V.C.; Jones, C.A. *Growth and Mineral Nutrition of Field Crops*; CRC Press: Boca Raton, FL, USA, 2010.
63. Majumdar, A.; Dubey, P.K.; Giri, B.; Moulick, D.; Srivastava, A.K.; Roychowdhury, T.; Bose, S.; Jaiswal, M.K. Combined effects of dry-wet irrigation, redox changes and microbial diversity on soil nutrient bioavailability in the rice field. *Soil Till. Res.* **2023**, *232*, 105752. [CrossRef]
64. Wang, J.; Pan, F.; Soininen, J.; Heino, J.; Shen, J. Nutrient enrichment modifies temperature-biodiversity relationships in large-scale field experiments. *Nat. Commun.* **2016**, *7*, 13960. [CrossRef]
65. Zhou, Z.; Wang, C.; Luo, Y. Meta-analysis of the impacts of global change factors on soil microbial diversity and functionality. *Nat. Commun.* **2020**, *11*, 3072. [CrossRef]
66. Heuck, C.; Weig, A.; Spohn, M. Soil microbial biomass C: N: P stoichiometry and microbial use of organic phosphorus. *Soil Biol. Biochem.* **2015**, *85*, 119–129. [CrossRef]
67. Majumdar, A.; Pradhan, N.; Sadasivan, J.; Acharya, A.; Ojha, N.; Babu, S.; Bose, S. Food degradation and foodborne diseases: A microbial approach. In *Microbial Contamination and Food Degradation*; Elsevier: Amsterdam, The Netherlands, 2018; pp. 109–148. [CrossRef]
68. Mu, C.; Zhang, T.; Zhang, X.; Li, L.; Guo, H.; Zhao, Q.; Cao, L.; Wu, Q.; Cheng, G. Carbon loss and chemical changes from permafrost collapse in the northern Tibetan Plateau. *J. Geophys. Res. Biogeosci.* **2016**, *121*, 1781–1791. [CrossRef]
69. Six, J.; Bossuyt, H.; Degryze, S.; Denef, K. A history of research on the link between (micro) aggregates, soil biota, and soil organic matter dynamics. *Soil. Till. Res.* **2004**, *79*, 7–31. [CrossRef]
70. Tisdall, J.M.; Oades, J.M. Organic matter and water-stable aggregates in soils. *J. Soil Sci.* **1982**, *33*, 141–163. [CrossRef]

71. Mu, C.; Abbott, B.W.; Zhao, Q.; Su, H.; Wang, S.; Wu, Q.; Zhang, T.; Wu, X. Permafrost collapse shifts alpine tundra to a carbon source but reduces N_2O and CH_4 release on the northern Qinghai-Tibetan Plateau. *Geophys. Res. Lett.* **2017**, *44*, 8945–8952. [CrossRef]
72. Bonde, T.A.; Schnurer, J.; Rosswall, T. Microbial biomass as a faction of potentially mineralizable nitrogen in soils from long-term field experiments. *Soil Biol. Biochem.* **1988**, *20*, 447–452. [CrossRef]
73. Wu, M.; Chen, S.; Chen, J.; Xue, K.; Chen, S.; Wang, X.; Chen, T.; Kang, S.; Rui, J.; Thies, J.E.; et al. Reduced microbial stability in the active layer is associated with carbon loss under alpine permafrost degradation. *Proc. Natl. Acad. Sci. USA* **2021**, *118*, e2025321118. [CrossRef]
74. Dong, X.; Man, H.; Liu, C.; Wu, X.; Zhu, J.; Zheng, Z.; Ma, D.; Li, M.; Zang, S. Changes in soil bacterial community along a gradient of permafrost degradation in Northeast China. *Catena* **2023**, *222*, 106870. [CrossRef]
75. Chapin, F.S.; Matson, P.A.; Vitousek, P. *Principles of Terrestrial Ecosystem Ecology*; Springer Science and Business Media: New York, NY, USA, 2011. [CrossRef]
76. Weedon, J.T.; Kowalchuk, G.A.; Aerts, R.; van Hal, J.; van Logtestijn, R.; Tas, N.; Röling, W.F.M.; van Bodegom, P.M. Summer warming accelerates sub-arctic peatland nitrogen cycling without changing enzyme pools or microbial community structure. *Glob. Chang. Biol.* **2012**, *18*, 138–150. [CrossRef]
77. Lawrence, D.M.; Koven, C.D.; Swenson, S.C.; Riley, W.J.; Slater, A.G. Permafrost thaw and resulting soil moisture changes regulate projected high-latitude CO_2 and CH_4 emissions. *Environ. Res. Lett.* **2015**, *10*, 094011. [CrossRef]
78. Li, S.; Fang, X.; Xiang, W.; Sun, W.; Zhang, S. Soil microbial biomass carbon and nitrogen concentrations in four subtropical forests in hilly region of central Hunan Province, China. *Sci. Silv. Sin.* **2014**, *50*, 8–16.
79. Kamimura, Y.; Hayano, K. Properties of protease extracted from tea-field soil. *Biol. Fert. Soils* **2000**, *30*, 351–355. [CrossRef]
80. Fontaine, S.; Barot, S. Size and functional diversity of microbe populations control plant persistence and long-term soil carbon accumulation. *Ecol. Lett.* **2005**, *8*, 1075–1087. [CrossRef]
81. Liu, W.; Jiang, Y.; Su, Y.; Smoak, J.M.; Duan, B. Warming affects soil nitrogen mineralization via changes in root exudation and associated soil microbial communities in a subalpine tree species *Abies fabri*. *J. Soil Sci. Plant Nut.* **2022**, *22*, 406–415. [CrossRef]
82. Hou, B.; Ma, F.; Wu, H.; Xin, S. Characteristics of soil nematodes communities at different succession stages of wetland in the Yellow River Delta, China, Chin. *Chin. J. Appl. Environ. Biol.* **2008**, *14*, 202–206. (In Chinese)